



UNIVERSITY OF LEEDS

This is a repository copy of *Thermoresponsive Polysarcosine-Based Nanoparticles*.

White Rose Research Online URL for this paper:

<http://eprints.whiterose.ac.uk/147208/>

Version: Accepted Version

Article:

Yu, H, Ingram, N orcid.org/0000-0001-5274-8502, Rowley, J orcid.org/0000-0001-6646-1676 et al. (4 more authors) (2019) Thermoresponsive Polysarcosine-Based Nanoparticles. *Journal of Materials Chemistry B*, 26. pp. 4217-4223. ISSN 2050-750X

<https://doi.org/10.1039/c9tb00588a>

© The Royal Society of Chemistry 2019. This is an author produced version of an article published in *Journal of Materials Chemistry B*. Uploaded in accordance with the publisher's self-archiving policy.

Reuse

Items deposited in White Rose Research Online are protected by copyright, with all rights reserved unless indicated otherwise. They may be downloaded and/or printed for private study, or other acts as permitted by national copyright laws. The publisher or other rights holders may allow further reproduction and re-use of the full text version. This is indicated by the licence information on the White Rose Research Online record for the item.

Takedown

If you consider content in White Rose Research Online to be in breach of UK law, please notify us by emailing eprints@whiterose.ac.uk including the URL of the record and the reason for the withdrawal request.



eprints@whiterose.ac.uk
<https://eprints.whiterose.ac.uk/>

**Thermoresponsive Polysarcosine-Based Nanoparticles**

Journal:	<i>Journal of Materials Chemistry B</i>
Manuscript ID	TB-ART-03-2019-000588.R1
Article Type:	Paper
Date Submitted by the Author:	26-Apr-2019
Complete List of Authors:	Yu, Huayang; University of Leeds, Chemistry Ingram, Nicola; St. James' Hospital, Leeds Institute of Biomedical and Clinical Sciences Rowley, Jason; University of Leeds, School of Chemistry Parkinson, Sam; University of Leeds, SCAPE Green, David; University of Leeds, School of Chemistry Warren, Nicholas; University of Leeds, Thornton, Paul; University of Leeds, School of Chemistry



Journal Name

ARTICLE

Thermoresponsive Polysarcosine-Based Nanoparticles

Received 00th January 20xx,
Accepted 00th January 20xx

DOI: 10.1039/x0xx00000x

www.rsc.org/

Huayang Yu^a, Nicola Ingram^b, Jason V. Rowley^a, Sam Parkinson^c, David C. Green^a, Nicholas J. Warren^c and Paul D. Thornton^{*a}

Polysarcosine holds great promise as an alternative to poly(ethylene glycol) for use within both biomedical and non-biomedical applications owing to its hydrophilicity and non-cytotoxicity, amongst other features. The grafting of a limited quantity of *N*-(2-hydroxypropyl)methacrylamide) to polysarcosine, for instance 3.5% of the total copolymer in terms of the number of repeat units, has a profound effect on the properties of the copolymer formed; polymer self-assembly to yield thermoresponsive nanoparticles can now be realised. Such nanoparticles are non-cytotoxic against a range of human breast cancer cell lines, able to withhold the therapeutic compound doxorubicin, and allow pronounced doxorubicin release in response to subtle thermal stimulation. This research informs of how the straightforward modification of polysarcosine with a nominal molar amount of poly(*N*-(2-hydroxypropyl)methacrylamide) can yield stimuli-responsive polymers that are suitable for use within controlled release applications.

Introduction

Polypeptoids can form effective components of biomaterials owing to their variable and controllable chemical functionality, thermal stability, non-cytotoxicity, potential degradability and low immunogenicity.¹ In particular, polysarcosine (PSar) holds outstanding promise as a biomedical polymer due to its hydrophilicity, the controllable manner in which its synthesis proceeds,^{2,3} and the exclusive H-bond acceptor repeat units that offer it resistance to protein fouling.⁴ Consequently, PSar offers a real alternative to poly(ethylene glycol) (PEG) for numerous applications,⁵ including its use as a non-fouling coating,⁶ and therapeutic protein conjugation.⁷ The precise control over PSar synthesis has enabled the accurate synthesis of block copolymers that contain PSar conjugated to other polypeptoids,⁸⁻¹⁰ poly(ϵ -caprolactone),^{11,12} tertiary amine-containing molecules,¹³ PEG,¹⁴ and poly(amino acids)/polyamides.¹⁵⁻¹⁷

There has been much recent interest in the application of PSar for the controlled release of therapeutic compounds. In such instances, PSar habitually forms the hydrophilic, and non-fouling, section of an amphiphilic block copolymer capable of forming nanoparticles in aqueous solution.¹⁸ Recent literature examples of PSar-based systems that have broad potential as

drug delivery/controlled release vehicles include the creation of amphiphilic block copolymers composed of PSar and poly(ϵ -caprolactone) that are capable of undergoing thermally-mediated self-assembly to bear a range of (nano)carriers,¹⁹ amphiphilic star-like copolymers consisting of PSar and Boc-protected polylysine, that undergo degradation in response to elevated glutathione concentration,²⁰ and very recently the creation of β -glucuronidase-responsive antibody drug conjugates (ADC) that feature PSar as a hydrophobicity masking entity within an ADC drug-linker platform.²¹ Recent work within our laboratory includes the creation of PSar-containing block copolymers, polymerised from a therapeutic initiator, that form enzyme-responsive nanoparticles,²² and the creation of poly(amino acid)-poly(ester) conjugates synthesised by glucosamine-initiated ring-opening polymerisation, that are susceptible to acid-mediated degradation.²³ Such promising results ensure that additional investigation into the use of PSar as a component within controlled release systems is of value.

The water-solubility of PSar ensures that polymer modification must be realised in order to create PSar-based nanoparticles in aqueous solution. Reversible addition-fragmentation chain-transfer (RAFT) polymerisation is an extensively exploited technique for the generation of amphiphilic block copolymers, and offers the opportunity to graft non-water-soluble oligomers/polymers to PSar, enabling the creation of thermoresponsive polymer nanoparticles.²⁴ Confirmation of nanoparticle formation, as RAFT polymerisation proceeds, may be achieved *in situ* using dynamic light scattering (DLS) measurements. Here, nanoparticle dimensions and dispersity are determined non-destructively, under normal conditions (i.e. without drying, extraction etc.), offering a convenient initial guide of the suitability of the block

^a School of Chemistry, University of Leeds, Leeds, United Kingdom, LS2 9JT, UK.

^b Leeds Institute of Biomedical and Clinical Sciences, Wellcome Trust Brenner Building, St James's University Hospital, Leeds, LS9 7TF, UK.

^c School of Chemical and Process Engineering, University of Leeds, Leeds, LS2 9JT, UK.

[†] Electronic Supplementary Information (ESI) available: ¹H NMR spectra, FTIR spectra, DLS spectra and cytotoxicity assay details.. See DOI: 10.1039/x0xx00000x

copolymer synthesised as a potential nanocarrier. The RAFT polymerisation of *N*-(2-hydroxypropyl)methacrylamide (HPMA) generates a non-immunogenic and non-toxic polymer,^{25,26} and a well-established route to PHPMA-based polymer nanoparticles is via RAFT aqueous dispersion polymerisation. Frequently, nanoparticles are produced by conducting this process in the presence of a PEG macro RAFT agent,²⁷ although recently, O'Reilly and co-workers described the preparation of a range of PSar-*b*-PHPMA copolymers capable of forming various morphologies dependant on the copolymer composition.²⁸ The number of non-biodegradable PHPMA repeat units within the block copolymer ranged between 100 and 400, and dictated the outcome of PSar₅₉-*b*-PHPMA_{*n*} self-assembly in aqueous solution. Although the drug delivery capabilities, and the thermoresponse, of the nanoparticles created were not reported, such materials may be considered appropriate for use in drug delivery applications if the molecular weight of the non-degradable PHPMA section within the copolymer can be limited to enable its clearance from the body, post-deployment.

We report the creation of thermoresponsive PSar-*b*-PHPMA nanoparticles designed to contain highly constrained molar amounts of PHPMA within the block copolymer composition. Nanoparticle formation was monitored *in situ*, and the polymer deemed most suitable for use as a potential drug delivery vehicle was advanced to doxorubicin (Dox) loading and release studies. The thermoresponse of the polymers was demonstrated by pronounced Dox release as a consequence of a moderate increase in solution temperature. Accordingly, the efficacy of the loaded nanoparticles against a range of breast cancer cell types was evaluated, and revealed that Dox-loaded nanoparticles were lethal against all breast cancer cell types tested, in marked contrast to unloaded non-cytotoxic nanoparticles. The reported polymers are thus highly-suited to the encapsulation and thermally-triggered release of molecular cargo, which may be applied for the eradication of breast cancer cells.

Experimental

Materials and Methods

Sarcosine (98 %) and *N*-boc-ethylenediamine hydrochloride (98 %) were purchased from Alfa Aesar. α -Pinene (98 %), trifluoroacetic acid (99%, extra pure), chloroform (99.9 %, extra dry over molecular sieve, stabilised, acroseal), tetrahydrofuran (99.5 %, Extra Dry, over Molecular Sieves) and buffer solution pH 5 (acetate buffer) were obtained from ACROS Organics. Triphosgene, triethylamine anhydrous and doxorubicin hydrochloride were obtained from Fluorochem. *n*-Hexane, ethanol absolute and dichloromethane were purchased from VWR International. Dimethyl sulfoxide (99.80 % D) was purchased from EURISO-TOP. Diethyl ether (analytical reagent grade) and triethylamine were obtained from Fisher Scientific. All other chemicals were obtained from Sigma-Aldrich

Chemical structures and functional groups were identified by Nuclear Magnetic Resonance (NMR, Bruker AVANCE III HD-400) and Attenuated Total Reflection (ATR-PLATINUM) Fourier Transform Infrared Spectroscopy (FTIR, BRUKER ALPHA). Particle size distribution of the products were measured via DLS (DLS, Malvern Zetasizer Nano ZSP). Scanning Electron Microscopy (SEM, FEI NanoSEM 450, elemental composition by energy-dispersive X-ray analysis) was employed to analyse size and topography of particle and particle surface. Melting point analysis was performed using a Stuart Scientific SMP 3 instrument. Elemental analysis of

nanoparticles was measured by Energy-Dispersive X-ray Spectroscopy). UV-vis spectroscopy (VARIAN 50 Probe UV-visible Spectrometer) was used to measure drug release from doxorubicin loaded polymer nanoparticles. The biocompatibility of the (loaded) polymers were measured via 3-(4,5-dimethylthiazol-2-yl)-2,5-diphenyltetrazolium bromide (MTT) assay / live-dead assay.

Copolymer molecular weights and molar mass dispersities were obtained by gel permeation chromatography (GPC) using an Agilent 1260 instrument equipped with 2 x mixed-C columns plus guard column and a refractive index detector. DMF containing 1.0 w/v % lithium bromide (LiBr) was used as eluent at a flow rate of 1.0 mL min⁻¹ and the temperature of the column oven and RI detector were set to 60 °C. A series of ten near-monodisperse poly(methyl methacrylate) standards (Mp ranging from 800 to 2,200,000 g mol⁻¹) were employed as calibration standards in conjunction with the RI detector for determining molecular weights.

Synthesis of Sarcosine NCA

Sarcosine NCA synthesis was conducted under a nitrogen atmosphere. 4.0 g of sarcosine and 14.0 mL of α -pinene were added to 60.0 mL of anhydrous tetrahydrofuran (THF). 10.0 g of triphosgene was dissolved in 10.0 mL of anhydrous THF and added dropwise to the reaction mixture. The mixture was stirred under reflux at 60 °C for 4.5 hours. The appearance of the resulting solution was brown-yellow. After rotary evaporation, brown precipitate and yellow solution were formed, before the products were stored under vacuum at 50 °C overnight. Consequently, brown solid formed that was dissolved in THF and added dropwise to cold *n*-hexane (recrystallisation). The recrystallisation procedure was performed two additional times before suction filtration was used to collect the products. The melting point was determined to be 104 °C – 104.6 °C, which is in agreement with prior studies.²⁹

Polymerisation of Sarcosine NCA from *N*-Boc-ethylenediamine

0.80 g of sarcosine NCA was dissolved in 3.0 mL of anhydrous DMF, maintained under constant nitrogen flow. Then, 0.01 g of *N*-boc-ethylenediamine hydrochloride was dissolved in 3.0 mL of anhydrous DMF before being added to the monomer solution. The polymerisation proceeded for four days until the products were isolated by polymer precipitation into 35 mL of cold diethyl ether. Polymer recovery has achieved by centrifugation for 30 minutes at 4,000 rev/min. Finally the products were dried under vacuum at room temperature overnight.

Boc Cleavage from PSar-Conjugated *N*-Boc-ethylenediamine

0.60 g of PSar-Conjugated *N*-Boc-ethylenediamine was dissolved in 6.0 mL of TFA, and the reaction was stirred overnight at room temperature. The solution was then added dropwise to cold diethyl ether, to isolate the product, which was recovered by centrifugation at 4000 rev/min for 30 minutes. Finally the products were dried in a vacuum oven overnight.

SCPDB Conjugation to Amine-Bearing Polysarcosine

Under a nitrogen atmosphere, 0.025 g of SCPDB and 0.50 g of the deprotected PSar were independently dissolved in 1.0 mL and 12.0 mL of anhydrous DCM, respectively. The solution containing PSar was then added dropwise to the SCPDB solution, and the mixture stirred overnight. Consequently, the solution was added dropwise to cold diethyl ether, resulting in the formation of a pink solid, which was isolated by centrifugation for 30 minutes at 4000 rev/min and then dried in a vacuum oven overnight. The product was washed with DCM before a second recrystallisation was performed, prior to product isolation and drying overnight under vacuum.

HPMA Polymerisation from the PSar-macro-RAFT Agent

Absolute ethanol and deionised water underwent nitrogenation overnight. 0.40 g of the PSar-macro-RAFT agent was dissolved in 2.0 mL of the absolute ethanol and followed by 30 minutes of ultrasonication. 0.015 g of APPH was dissolved in 10.0 mL of deionised water. Next, 0.082 g of the HPMA monomer was added to the macro-RAFT agent solution, before the AAPH solution, in addition to 3.0 mL of deionised water, were added. The mixture was stirred and stirred and degassed with nitrogen for 30 minutes before the mixture was heated in an oil bath for 4 hours at 55 °C. Every hour 1.5 mL of the reaction mixture was removed from the polymerisation, and DLS analysis was performed. Finally, the product was dialysed for six days, freeze dried for 2 days and stored in a desiccator.

Results and discussion

N-Boc-ethylenediamine was selected as a dual initiator for NCA ROP, and upon Boc group cleavage, RAFT polymerisation. The primary amine presented by the initiator enables the ROP of sarcosine NCA, yielding Boc group protected PSar (Scheme 1a). Boc cleavage was achieved using TFA (Scheme 1b), yielding a range of homopolymers that contained PSar with chain lengths of 58 and 137 repeat units. The primary amine group liberated was used for RAFT agent (4-cyano-4-(phenylcarbonothioylthio) pentanoic acid *N*-succinimidyl ester (SCPDB)) conjugation (Scheme 1c), before HPMA polymerisation was conducted in an ethanol/water mixture to yield a range of block copolymers (Scheme 1d).

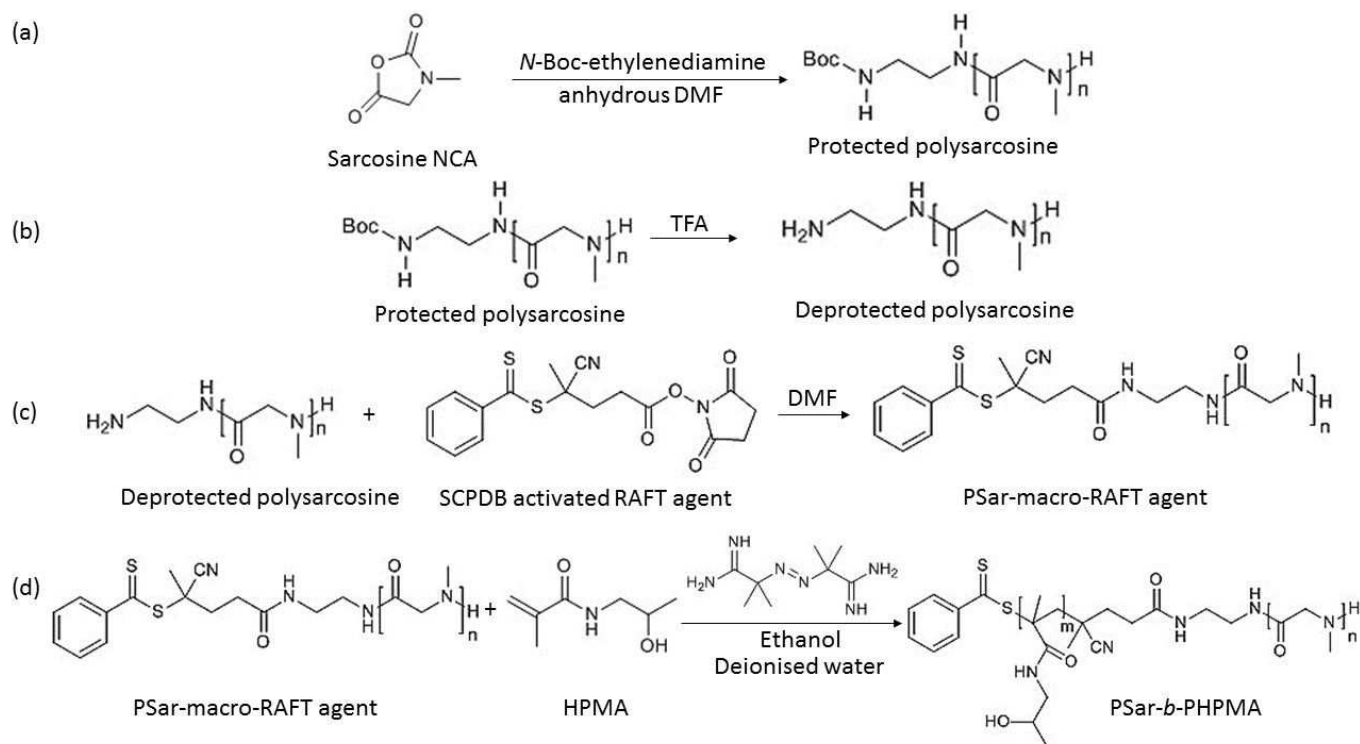
Progress towards the desired block copolymers was monitored by FTIR (Figure S1). The secondary amide peak corresponding to PSar is present throughout the synthesis, but the ester peak attributed to the presence of the Boc protecting group (1227 cm⁻¹) disappeared as expected upon Boc group cleavage. The grafting of the RAFT agent to polysarcosine resulted in the emergence of peaks representative of aromatic groups in the 900 cm⁻¹ to 500 cm⁻¹ region. The peak corresponding to the nitrile functional group is visible, however, this peak is very weak since there is designed to be only a single nitrile group per polymer chain. The FTIR spectrum of the final product, revealed the presence of the alcohol functional group (3486 cm⁻¹, merged with secondary amine). The structures of all (macro)molecules formed were confirmed by ¹H NMR spectroscopy (Figures S2-S17 and S20-S23).

During each polymerisation, nanoparticle formation was tracked by DLS. Initially, two block copolymers (PSar₅₈-*b*-PHPMA₈₂ and PSar₁₃₇-*b*-PHPMA₂₇₃, where the number of repeat units represent complete monomer conversion to the final polymer after 4-hour polymerisation) were synthesised and examined (Table 1, DLS data presented in Figures S24 and S25). Nanoparticle sizes increased with time following a non-linear relationship, suggesting nanoparticle growth was mostly complete after approximately 3 hours. In addition, the particles became excessively large, with the exception of PSar₁₃₇-*b*-PHPMA₂₇₃ when polymerised for up to 2 hours. Consequently, it was decided that SCPDB conjugated to PSar (137 repeat units) is a suitable macroinitiator for HPMA polymerisation, but the extent of HPMA polymerisation must be limited to yield desirable particles of less than 200 nm hydrodynamic diameter. A third block copolymer, PSar₇₈-*b*-PHPMA₁₃₀ after four hours polymerisation, was also produced and exhibited *in situ* particle formation during HPMA polymerisation (Table S1). However, this

polymer was not progressed due to relatively large hydrodynamic diameters/PDI values obtained for the particles formed.

Studies were undertaken whereby two target polymers, PSar₁₃₆-*b*-PHPMA₅₃ and PSar₁₃₆-*b*-PHPMA₁₄, were produced over a 4-hour period, with polymer being isolated from the reaction vessel every hour. Polymer self-assembly by coacervation was undertaken and the nanoparticles formed analysed by DLS. Whilst PSar₁₃₆ was unable to self-assemble to form nanoparticles in aqueous solution, SCPDB conjugation to PSar₁₃₆ resulted in the formation of nanoparticles with a mean diameter of 114 nm and a PDI value of 0.454. Subsequent HPMA polymerisation from the macroinitiator resulted in the creation of nanoparticles of increased diameter (Table 2). Nanoparticle stability, in terms of both size and dispersity, is provided in Table 3 (particle diameter) and Table S2 (particle dispersity). The dimensions of many of the nanoparticle samples formed rendered many suitable candidates for use as potential drug delivery vehicles. Nanoparticles isolated from PSar₁₃₆-*b*-PHPMA₁₄ and PSar₁₃₆-*b*-PHPMA₅₃ polymerisations after 2-hours were deemed the most appropriate to be advanced to Dox release studies. The structures of these polymers were found to be PSar₁₃₆-*b*-PHPMA₅ and PSar₁₃₆-*b*-PHPMA₂₁, respectively, as determined by ¹H NMR spectroscopy (Figures S16 and S17). The molecular weights and dispersity values of the polymers were found to be 11,600 g.mol⁻¹ and 1.26, respectively, for PSar₁₃₆-*b*-PHPMA₅, and 14,000 g.mol⁻¹ and 1.07, respectively, for PSar₁₃₆-*b*-PHPMA₂₁, as determined by GPC. SEM studies revealed the formation of discrete nanoparticles from PSar₁₃₆-*b*-PHPMA₅ and PSar₁₃₆-*b*-PHPMA₂₁ copolymers (Figure 2 and Figure S26, respectively). Energy dispersive X-ray analysis revealed the presence of sulfur only where particles were found, confirming the retention of the RAFT agent and successful polymerisation (Figure S27).

Although the particles disclosed in this paper may readily be applied as materials that enable the controlled release of a range of molecular cargoes, the loading, and release, of an anticancer drug (Dox) into/from the particles was selected for further evaluation. The particles are deemed suitable candidates as drug delivery vehicles owing to their limited non-degradable polymer content, which is restricted to five repeat units on average per polymer chain in the case of PSar₁₃₆-*b*-PHPMA₅. Dox loading into polymer nanoparticles was achieved by 'dropping in' a solution of polymer dissolved in DMF to vigorously stirred phosphate buffered saline (PBS) solution that contained Dox.³⁰ 97.9% (0.294 mg) of Dox added was loaded within 2 mg of PSar₁₃₆-*b*-PHPMA₅ particles maintained in pH 7.4 solution and 96.8% (0.291 mg) of Dox added was loaded within 2 mg of PSar₁₃₆-*b*-PHPMA₅ added was loaded within 2 mg of PSar₁₃₆-*b*-PHPMA₂₁ particles maintained in pH 7.4 solution and 96.5% (0.289 mg) Dox added was loaded within 2 mg of particles maintained in pH 5 solution. 97.2% (0.292 mg) of Dox added was loaded within 2 mg of PSar₁₃₆-*b*-PHPMA₂₁ particles maintained in pH 7.4 solution and 96.5% (0.289 mg) Dox added was loaded within 2 mg of PSar₁₃₆-*b*-PHPMA₂₁ particles maintained in pH 5 solution. PSar₁₃₆-*b*-PHPMA₅ yielded Dox-loaded particles of 161 nm (PDI = 0.240) and PSar₁₃₆-*b*-PHPMA₂₁ yielded Dox-loaded particles of 159 nm (PDI = 0.254). The PSar₁₃₆-*b*-PHPMA₅ particles were found to be stable when maintained in PBS buffer at 25 °C for at least 21 days, decreasing in hydrodynamic diameter insignificantly to 156 nm (PDI = 0.189, Table S3). PSar₁₃₆-*b*-PHPMA₅ particles stored in PBS buffer at 37 °C



Scheme 1. The route to PSar-*b*-PHPMA. a) The synthesis of Boc protected PSar. b) Boc group cleavage to provide primary amine functionality to PSar. c) RAFT agent conjugation to PSar. d) RAFT polymerisation of HPMA from PSar.

decreased in hydrodynamic diameter from 130 nm to 129 nm after 21 days (Table S4). However, in this instance a second peak formed over time that, after 21 days, was representative of particles that possess a hydrodynamic diameter of 31 nm and represented 6.1% of the total sample measured. The overall PDI of the sample was

Table 1. Nanoparticle size and PDI values for nanoparticles formed *in situ*.

Duration	PSar ₅₈ - <i>b</i> -PHPMA ₈₂ (nm)	PDI	PSar ₁₃₇ - <i>b</i> -PHPMA ₂₇₃ (nm)	PDI
1 hour	393	0.409	129	0.326
2 hours	544	0.626	226	0.345
3 hours	554	0.174	365	0.306
4 hours	488	0.481	325	0.331

Table 2. Nanoparticle size and PDI values for nanoparticles formed from PSar₁₃₆-*b*-PHPMA₁₄ and PSar₁₃₆-*b*-PHPMA₅₃ following polymer coacervation.

Duration	PSar ₁₃₆ - <i>b</i> -PHPMA ₁₄	PDI	PSar ₁₃₆ - <i>b</i> -PHPMA ₅₃	PDI
1 hour	144	0.176	149	0.129
2 hours	151	0.559	178	0.147
3 hours	247	0.336	195	0.058
4 hours	315	0.121	272	0.007

therefore relatively large (0.437), and indicates that Dox release occurs to a limited extent when PSar₁₃₆-*b*-PHPMA₅ particles are stored at 37 °C for extended periods. Dox release from PSar₁₃₆-*b*-PHPMA₅ particles independently maintained in PBS solution (pH 7.4) and acetate buffer (pH 5) at 37 °C, under steady agitation, revealed that at 37 °C, both polymers released Dox slowly, with 20 % of Dox released from PSar₁₃₆-*b*-PHPMA₅ at pH 5 and 4 % of loaded Dox released from the same polymer after 18 days incubation at pH 7.4

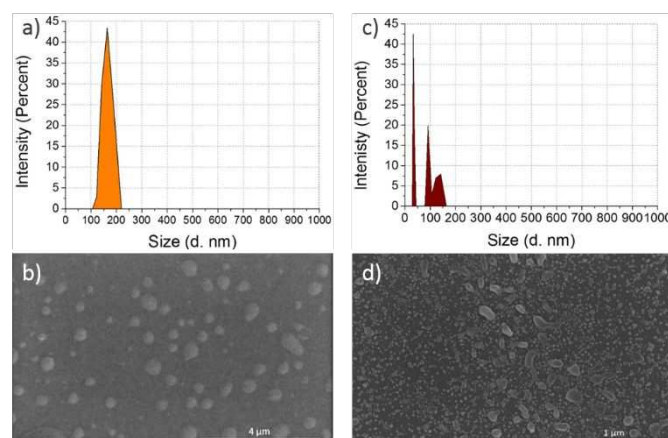


Figure 2 a) Particle size determination of PSar₁₃₆-*b*-PHPMA₅ via DLS, b) SEM micrograph of PSar₁₃₆-*b*-PHPMA₅ nanoparticles. Scale bar represents 4 μm. c) Particle size determination and d) SEM images corresponding to Dox-loaded nanoparticles formed from PSar₁₃₆-*b*-HPMA₅ that had been subjected to heating to 50 °C for 24 hours. Scale bar represents 4 μm.

Table 3 A comparison of stability of the nanoparticles formed upon polymer precipitation at hourly intervals during the synthesis of PSar₁₃₆-*b*-PHPMA₁₄ and PSar₁₃₆-*b*-PHPMA₅₃.

Copolymer Target	Size (nm)		
	After 24 hours	After 14 days	After 21 days
PSar₁₃₆-<i>b</i>-PHPMA₁₄			
1h	187	160	178
2h	207	135	156
3h	234	171	195
4h	284	271	293
PSar₁₃₆-<i>b</i>-PHPMA₅₃			
1h	154	151	159
2h	197	140	148
3h	148	169	163
4h	288	276	288

(Figure 3). 10% (pH 5) and 2% (pH 7.4) of loaded Dox was released from PSar₁₃₆-*b*-PHPMA₂₁ after 18 days incubation (Figure S28). Greater Dox release occurred from nanoparticles stored in pH 5 solution compared to those stored in pH 7.4 solution, which may be explained by the primary amine of Dox being protonated when in pH 5 solution, enhancing the water solubility of the drug and aiding its release into acidic solution.

Subsequent heating of both sets of nanoparticles to 50 °C was done to assess their thermoresponse. Enhanced Dox release (91% in pH 5 solution, 83% in pH 7.4 solution) of Dox from PSar₁₃₆-*b*-PHPMA₅ particles occurred following re-assessment after a further 7 days of heating at the elevated temperature. PSar₁₃₆-*b*-PHPMA₂₁ particles also demonstrated enhanced Dox release upon heating at 50 °C, but in this case 30% (pH 5) and 16% (pH 7.4) of payload was released from the nanoparticles following re-assessment after 7 days of heating. The slower rate of Dox release from PSar₁₃₆-*b*-PHPMA₂₁ may

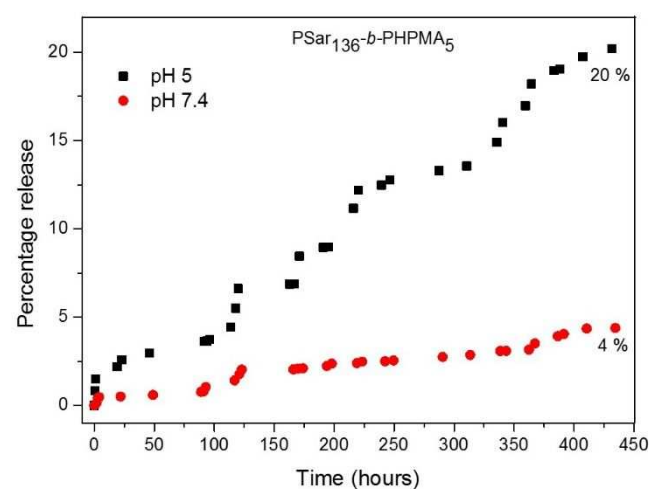


Figure 3 Doxorubicin release from PSar₁₃₆-*b*-PHPMA₅ at pH 5 and pH 7.4.

Table 4. A comparison of Dox loaded and unloaded PSar₁₃₆-*b*-PHPMA₅ nanoparticle sizes at room temperature 37 °C, and 50 °C.

Polymer	Size (nm)	PDI
PSar ₁₃₆ - <i>b</i> -PHPMA ₅ without doxorubicin loaded at room temperature	166	0.218
At 37 °C	164	0.261
At 50 °C	132	0.215
PSar ₁₃₆ - <i>b</i> -PHPMA ₅ with doxorubicin loaded at room temperature	161	0.240
At 37 °C	130	0.389
At 50 °C	91	0.468

be assigned to the increased length of the thermoresponsive PHPMA section within the composition. Altering the PHPMA block length to manipulate drug release extent/rate is a feature that may be further exploited. The critical temperature at which Dox release from PSar₁₃₆-*b*-PHPMA₅ nanoparticles is triggered was then determined. Initially, DLS studies revealed that the size of unloaded nanoparticles did not change significantly upon increasing the solution temperature from 25 °C (166 nm) to 37 °C (164 nm) (Table 4). Upon increasing the temperature to 50 °C, the particle size decreased to 132 nm. All PDI values for the unloaded nanoparticles were less than 0.3, signifying that the nanoparticles were stable at room temperature, 37 °C and 50 °C. PSar₁₃₆-*b*-PHPMA₅ nanoparticles loaded with Dox had a hydrodynamic diameter of 161 nm in aqueous solution at 25 °C. The Dox-loaded nanoparticle size decreased from 161 nm to 130 nm as the temperature was increased to 37 °C. Upon further solution temperature increase to 50 °C, the particle size decreased further to 91 nm. This dramatic decrease in nanoparticle diameter, and the consequent expulsion of Dox from the nanoparticles, is proposed to be the reason for extensive Dox release at 50 °C. The PDI values of the Dox-loaded nanoparticles at 37 °C (0.389) and 50 °C (0.468) were above 0.3; such instability is likely to be due to the release of Dox.

The change in the morphology of the nanoparticles that contained Dox could clearly be evidenced by SEM analysis, after

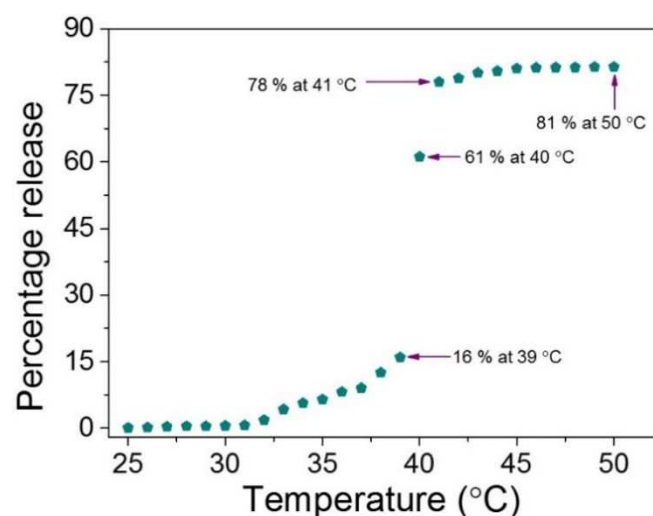


Figure 4. The temperature-dependent release of Dox from PSar₁₃₆-*b*-PHPMA₅ nanoparticles upon incremental solution temperature increase.

ARTICLE

Journal Name

heating the nanoparticles to 50 °C for 24 hours (Figure 2d). Less spherical, more elongated, particles were observed by SEM analysis, further confirming that a thermally-induced nanoparticle transition had occurred. Smaller particles (34 nm) were observed in post-heated samples that may be assigned to be released Dox aggregates. The release of Dox from PSar₁₃₆-*b*-PHPMA₅ nanoparticles was then monitored in response to incremental PBS solution temperature increases whereby the solution temperature was raised by 1 °C, the solution was maintained at the increased temperature for 24 hours, and the amount of Dox released at the increased temperature was measured (Figure 4). Dox release occurred slowly and steadily to 16 % as the solution temperature was increased from 25 °C to 39 °C over 360 hours. At this point the percentage of Dox released increased markedly to 78 % at 41 °C, signifying that the critical temperature for Dox burst release, and that the likely solution glass transition temperature of the hydrated block copolymer is between 39 °C and 41 °C. A more detailed study in which the loaded nanoparticles were monitored at 40 °C for 24 hours confirmed that 62.4% Dox release was achieved by heating the nanoparticles to 40 °C for 24 hours (Figure S29). This offers validation that the reported nanoparticles are pharmacologically relevant; payload release can be actuated by nanoparticle heating to a temperature that is not detrimental to cell survival.

Pharmacological studies were undertaken whereby the cytotoxicity of the nanoparticles formed from PSar₁₃₆-*b*-PHPMA₅ were assessed on MCF-7 breast cancer cells, triple-negative breast cancer cells (MDA-MB-231), and Her2-enriched (ER and PR negative) breast cancer cells (MDA-MB-453), to assess the capability of the materials to potentially treat chemo-refractory disease. Free Dox was used as a positive control (Tables S5 and S6). In all instances, the polymer nanoparticles were found to cause negligible cell death at both 37 °C and at 41 °C, validating the non-cytotoxicity of the polymers produced (Figure 5). Dox-loaded nanoparticles were then assessed against the three same cell lines; in each instance pronounced cell death occurred that became progressively greater with enhanced polymer concentration. It may be hypothesised that the nanoparticles are of sufficiently small dimensions to undergo endocytosis both at the lower and elevated temperature, and that Dox leakage from the nanoparticles is sufficiently significant to cause cell death following nanoparticle uptake.

Conclusions

Combining NCA ROP and RAFT polymerisation is a viable route to the creation of amphiphilic block copolymers that are thermoresponsive. The synthesis of a PSar-*b*-PHPMA in a water/ethanol mixture leads to the *in situ* formation of particles, as assessed by DLS. Using DLS in this manner enables the elucidation of the ideal composition of PSar-*b*-PHPMA for the creation of suitably sized, stable, nanoparticles for controlled release applications. Modifying PSar with a very moderate amount of PHPMA has a profound effect on the copolymer formed, which is capable of thermoresponsive nanoparticle formation in aqueous solution. PSar₁₃₆-*b*-PHPMA₅ self-assembly in the presence of Dox yields drug-loaded nanoparticles, and Dox release from the nanoparticles can be actuated by an increase in environmental temperature to 41 °C. Such nanoparticles are non-cytotoxic against the three breast cancer cell lines tested, in contrast to Dox-loaded nanoparticles which instigated pronounced cell death in each case. Consequently, the nanoparticles disclosed have potential

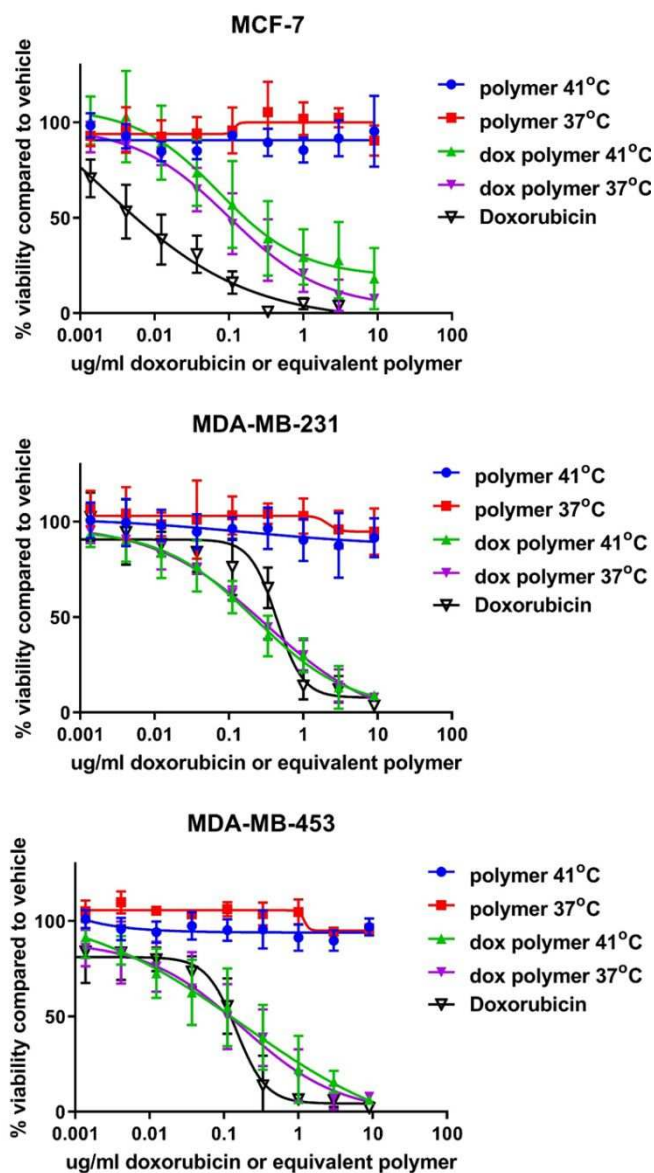


Figure 5. Cytotoxicity of PSar₁₃₆-*b*-PHPMA₅ either empty (polymer only) or loaded with doxorubicin (dox polymer) on three breast cancer cell lines. Serial dilutions of polymer or dox polymer were incubated with MCF-7, MDA-MB-231 (triple negative) or MDA-MB-453 (double negative) cell lines for 72 hours either with or without incubation of the cells at 41 °C for 40 minutes within the first hour of incubation. Graphs of the mean and standard deviation from 3 independent experiments are fitted with a four parameter log inhibitor curve.

application for the thermally-triggered release of guest molecules to external solution, and the encapsulation, distribution, and release of Dox to breast cancer cells as a mode of therapeutic delivery.

Conflicts of interest

There are no conflicts to declare.

Notes and references

30 M. Khuphe and P. D. Thornton, *Macromol. Chem. Phys.*, 2018, **219**, 1800352.

- 1 B. A. Chan, S. T. Xuan, A. Li, J. M. Simpson, G. L. Sternhagen, T. Y. Yu, O. A. Darvish, N. S. Jiang and D. H. Zhang, *Biopolymers*, 2018, **109**, e23070.
- 2 Y. L. Hu, Y. Q. Hou, H. Wang and H. Lu, *Bioconjugate Chemistry*, 2018, **29**, 2232.
- 3 B. Weber, A. Birke, K. Fischer, M. Schmidt and Matthias Barz, *Macromolecules*, 2018, **51**, 2653.
- 4 R. G. Chapman, E. Ostuni, M. N. Liang, G. Meluleni, E. Kim, L. Yan, G. Pier, H. S. Warren and G. M. Whitesides, *Langmuir*, 2001, **17**, 1225.
- 5 D. Huesmann, A. Sevenich, B. Weber and M. Barz, *Polymer*, 2015, **67**, 240.
- 6 K. H. A. Lau, C. Ren, T. S. Sileika, S. Hyun Park, I. Szeleifer and P. B. Messersmith, *Langmuir*, 2012, **28**, 16099.
- 7 Y. Hu, Y. Hou, H. Wang and H. Lu, *Bioconjugate Chem.*, 2018, **29**, 2232.
- 8 C. Fetsch, A. Grossmann, L. Holz, J. F. Nawroth and R. Luxenhofer, *Macromolecules*, 2011, **44**, 6746.
- 9 N. Gangloff, M. Höferth, V. Stepanenko, B. Sochor, B. Schummer, J. Nickel, H. Walles, R. Hanke, F. Würthner, R. N. Zuckermann and R. Luxenhofer, *Biopolymers*, 2019, DOI: 10.1002/bip.23259.
- 10 C. Fetsch, S. Flecks, D. Gieseler, C. Marschelke, J. Ulbricht, K.-H. van Pée and Robert Luxenhofer, *Macromol. Chem. Phys.*, 2015, **216**, 547.
- 11 S. Cui, X. Pan, H. Gebru, X. Wang, J. Liu, J. Liu, Z. Li and K. Guo, *J. Mater. Chem. B*, 2017, **5**, 679.
- 12 Y. Deng, T. Zou, X. Tao, V. Semetey, S. Trepout, S. Marco, J. Ling and M.-H. Li, *Biomacromolecules*, 2015, **16**, 3265.
- 13 A. Doriti, S. M. Brosnan, S. M. Weidner and H. Schlaad, *Polym. Chem.*, 2016, **7**, 3067.
- 14 X. Tao, C. Deng and Jun Ling, *Macromol. Rapid Commun.*, 2014, **35**, 875.
- 15 J. Du, C. Tian, Y. Liu, J. Ling and Y. Wang, *Colloids Surf. B*, 2015, **130**, 31.
- 16 A. Birke, J. Ling and M. Barz, *Prog. Polym. Sci.*, 2018, **81**, 163.
- 17 C. J. Kim, M. Ueda, T. Imai, J. Sugiyama and S. Kimura, *Langmuir*, 2017, **33**, 5423.
- 18 A. Birke, D. Huesmann, A. Kelsch, M. Weilbacher, J. Xie, M. Bros, T. Bopp, C. Becker, K. Landfester and M. Barz, *Biomacromolecules*, 2014, **15**, pp 548.
- 19 Y. Deng, T. Zou, X. Tao, V. Semetey, S. Trepout, S. Marco, J. Ling and Min-Hui Li, *Biomacromolecules*, 2015, **16**, pp 3265.
- 20 R. Holm, B. Weber, P. Heller, K. Klinker, D. Westmeier, D. Docter, R. H. Stauber and M. Barz, *Macromolecular Bioscience*, 2017, **17**, 1600514.
- 21 W. Viricel, G. Fournet, S. Beaumel, E. Perrial, S. Papot, C. Dumontet and B. Joseph, *Chem. Sci.* 2019, DOI:10.1039/C9SC00285E.
- 22 M. Khuphe, A. Kazlauciuonas, M. Huscroft and P. D. Thornton, *Chem. Commun.*, 2015, **51**, 1520.
- 23 M. Khuphe, C. S. Mahon and P. D. Thornton, *Biomater. Sci.*, 2016, **4**, 1792.
- 24 C. Q. Gao, H. Zhou, Y. Q. Qu, W. Wang, H. Khan W. Q. Zhang, *Macromolecules*. 2016, **49**, 3789.
- 25 Q. S. Yu, C. Y. Dong, J. J. Zhang, J. Y. Shi, B. Jia, F. Wang and Z. Gan, *Polym. Chem.*, 2014, **5**, 5617.
- 26 N. J. Warren, O. O. Mykhaylyk, D. Mahmood, A. J. Ryan and S. P. Armes, *J. Am. Chem. Soc.*, 2014, **136**, 1023.
- 27 N. J. Warren and S. P. Armes, *J. Am. Chem. Soc.*, 2014, **136**, 10174.
- 28 S. Varlas, P. G. Georgiou, P. Bilalis, J. R. Jones, N. Hadjichristidis and R. K. O'Reilly, *Biomacromolecules*, 2018, **19**, 4453.
- 29 K. Klinker, R. Holm, P. Heller and Matthias Barz, *Polym. Chem.*, 2015, **6**, 4612.

